JOURNAL OF SOLID STATE CHEMISTRY 46, 23–40 (1983)

Microdomain Texture and Oxygen Excess in the Calcium–Lanthanum Ferrite: $Ca_2LaFe_3O_8$

MIGUEL A. ALARIO-FRANCO,* MARÍA JESÚS R. HENCHE, MARÍA VALLET, AND JOSÉ M. G. CALBET

Departamento de Química Inorgánica, Facultad de Ciencias Químicas, Universidad Complutense, Ciudad Universitaria, Madrid 3, and, Instituto "Elhuyar," CSIC, Madrid 6, Spain

AND JEAN-CLAUDE GRENIER, ALAIN WATTIAUX, AND PAUL HAGENMULLER

Laboratoire de Chimie du Solide du CNRS, Université de Bordeaux I, 351, cours de la Libération, 33405 Talence Cedex, France

Received May 18, 1982

The analysis by TEM and electron diffraction of the anion-deficient perovskite $Ca_2LaFe_3O_8$ confirms the model previously proposed by J. C. Grenier *et al.* (*Mater. Res. Bull.* **11**, 1219 (1976)) with a structure intermediate between perovskite and brownmillerite. The unit cell parameters are $\sim\sqrt{2}a_c$, $3a_c$, $\sqrt{2}a_c$ (where a_c is the cubic perovskite unit cell parameter). However, the unit cell is sometimes doubled along the *b* axis. When the sample is treated in air at temperatures around 1400°C, an oxidation process is observed and the unit cell becomes cubic (a_c = 3.848(3) Å). Nevertheless, electron diffraction investigations suggest the existence of a much more complex situation in which three-dimensional microdomains intergrow within one crystal. Each of these microdomains appears to have a structure clearly related to the low-temperature sample, but the superstructure is randomly found along each of the three cubic subcell directions (i.e., the unit cell $\sqrt{2}a_c$, $\sqrt{2}a_c$, $3a_c$ alternates randomly with $3a_c$, $\sqrt{2}a_c$, $\sqrt{2}a$, and with $\sqrt{2}a_c$, $3a_c$, $\sqrt{2}a_c$). High-resolution electron microscopy allows one to ascertain this *microdomain texture* of the real crystal.

Introduction

There are several ways for a metal oxide to change its composition. One may mention, for instance, the following: *Point defects*, probably operative when the compositional variations are small, as, for example, in the alkaline-earth metal oxides (*1*). *Defect complexes*, as, for example, in UO_{2+x} and other fluorite-type oxides (*2*). *Crystallographic shear planes*, as in TiO_{2-x} (*3*), WO_{3-x} (*4*), or in its two-dimensional manifestation in so-called column structures (*5*), formerly denominated "block structures" (*6*). *Intergrowth* of two or more basic structural motifs in various proportions, as observed in phases intermediate between the perovskite and brownmillerite structural types. Such phases have recently been discovered by Grenier *et al.* (*7, 8*). In these materials, perovskite-like octahedra

* Author to whom correspondence should be addressed.

0022-4596/83/010023-18$03.00/0

layers form an intergrowth with tetrahedra layers in ordered sequences whose general formula is

$$A_nM_nO_{3n-1} \Leftrightarrow AMO_{3-y}, \qquad \text{with } y = 1/n.$$

The two extreme terms of the series are:

—for $n = 2$ brownmillerite (*9, 10*), where the sequence of octahedra (O) and tetrahedra (T) layers is . . .OTOT'OTOT'. . .[1];

—for $n = \infty$, where no tetrahedra layers are present, the sequence is then . . .OOO. . ., corresponding to the cubic perovskite structure.

Idealized polyhedral models of these structures are represented in Figs. 1a and b.

Within the structural family, other known terms correspond to $n = 5/2$ or 4 (*11*). The present paper is devoted to materials whose compositions are close to $n = 3$, i.e., to $Ca_2LaFe_3O_8$.

It came out from a previous work (*12*) that this compound has an orthorhombic unit cell whose parameters can be expressed as a function of the cubic perovskite cell parameter a_c by $a_o \simeq a_c\sqrt{2}$, $b_o \simeq 3a_c$, and $c_o \simeq a_c\sqrt{2}$.[2] It is characterized by a . . .OOTOOT. . . sequence (Fig. 1c).

It was also observed that the mixed calcium–lanthanum ferrite $Ca_2LaFe_3O_8$, when heated in air at 1400°C, did gain a slight oxygen excess over the stoichiometric formula and, instead of orthorhombic, it was cubic according to its powder X-ray diffraction pattern (*12*). Taking into account the general characteristics of such an ordered intergrowth (*8, 11*), it could be expected that an oxygen excess was accommodated by a simple rearrangement and change in the separation between the tetrahedra layers. However, as reported below, an electron microscopy and diffraction study of the oxidized materials shows that under these circumstances compositional variations are accommodated by means of the formation of three-dimensional microdomains.

[1] For an explanation of the difference between T and T' see below and Fig. 1.

[2] Subindexes o and c refer to the orthorhombic and cubic unit cells, respectively. Subindex B refers to the brownmillerite-type unit cell.

Experimental

The calcium lanthanum ferrite was prepared from the stoichiometric mixture ($4CaCO_3$, La_2O_3, $6Fe(NO_3)_3$, $9H_2O$), but in order to obtain homogeneous samples the starting materials were dissolved in dilute nitric acid. The nitrates were then decomposed at 800–1000°C. Finally, after grinding several times, they were fired at 1300°C.

The low-temperature sample (L.T.) was annealed at 1100°C under controlled oxygen pressure in an argon atmosphere ($p_{O_2} \simeq 10^{-7}$ atm) in order to prevent the formation of iron(IV).

The high-temperature sample (H.T.) was obtained by annealing at 1400°C in air for 1 day followed by quick-quenching down to room temperature.

The samples were characterized by powder X-ray diffraction (Guinier–Hägg pattern with Cu$K\alpha$ radiation) and chemical analysis (determination of the average oxidation state of iron by $K_2Cr_2O_7$ after dilution in 3 N HCl with an excess of Mohr's salt).

Electron microscopy and diffraction were performed on a Siemens Elmiskop 102. The samples were ultrasonically dispersed in n-butanol and then transferred to carbon-coated copper grids.

Results

Low-Temperature Sample: $Ca_2LaFe_3O_8$ (L.T.)

According to the X-ray diffraction work (*8*), this reduced sample appears to have an orthorhombic cell related to a perovskite cell. The unit cell parameters are a_o =

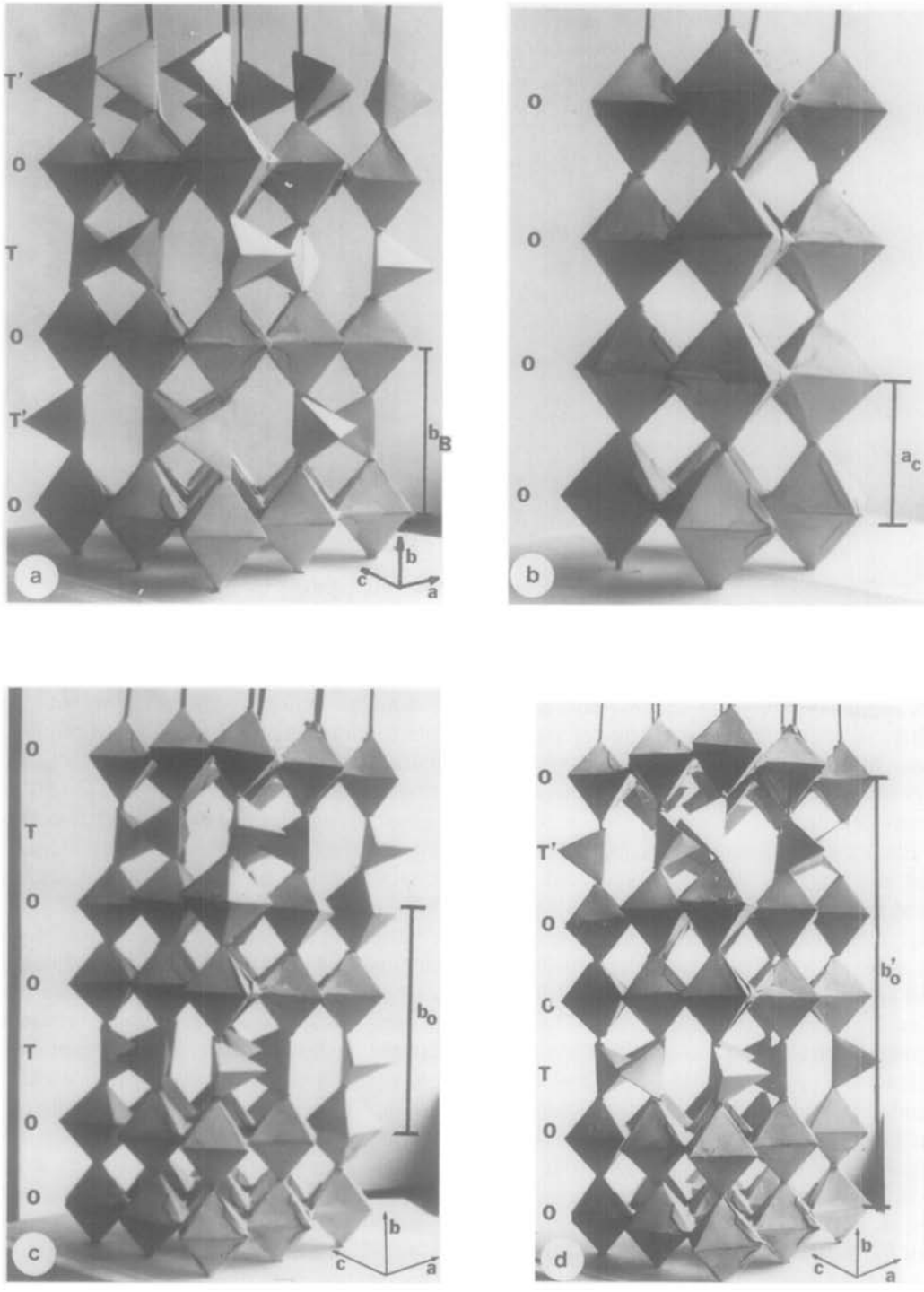

FIG. 1. Idealized polyhedral models of the following structures: (a) brownmillerite; (b) perovskite; (c) polytype I of $Ca_2LaFe_3O_8$; and (d) polytype II of $Ca_2LaFe_3O_8$.

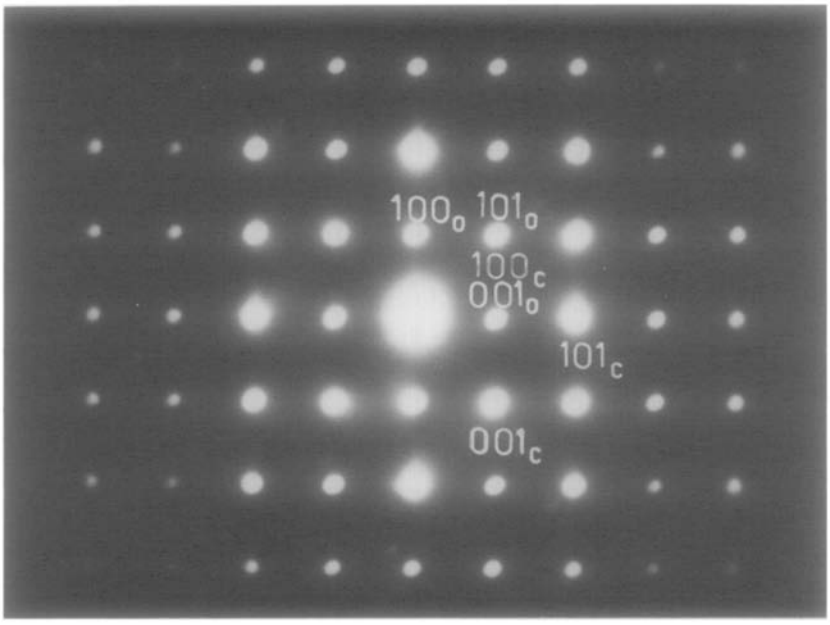

FIG. 2. Electron diffraction pattern of the low-temperature orthorhombic sample. Zone axis $[010]_o \leftrightarrow [010]_c$ (o ≡ orthorhombic cell of Grenier *et al.* (*12*); c = cubic perovskite cell).

5.464(3), b_o = 11.29(1), and c_o = 5.563(3) Å, i.e., approximately $a_c\sqrt{2}$, $3a_c$, and $a_c\sqrt{2}$, where a_c is the cubic perovskite cell parameter. Moreover, the chemical analysis of this sample does not reveal the presence of tetravelent iron.

Electron diffraction work corroborated that the majority of the crystals did conform to the model of Grenier *et al.* (*8*). In Fig. 2, the electron diffraction pattern can be indexed as $[010]_o$, equivalent to $[010]_c$, and clearly shows the orthorhombic distortion. By electron diffraction c/a = 1.01, in agreement with the ratio obtained by X-ray diffraction (c/a = 1.018). On the other hand, Figs. 3 to 6 show a series of reciprocal lattice sections containing the b_o axis. Figure 3, corresponding to the $[10\bar{3}]_o$ zone axis, equivalent to the $[10\bar{2}]_c$ zone axis, and Fig. 4, corresponding to the $[10\bar{2}]_o$, equivalent to $[10\bar{3}]_c$, show that the b_o^* axis presents a threefold superlattice with respect to the cubic perovskite a_c^* axis. Some crystals, however, did show a marked streaking along the b_o^* axis, suggesting the existence of some disorder in the stacking of the atomic planes along the real b_o direction. Figure 5a gives a clear example of the streaking, and the corresponding disorder is observed in Fig. 5b; both pictures correspond to the $[10\bar{1}]_o$ zone axis, equivalent to the $[100]_c$ zone axis. Finally, Fig. 6 shows $[100]_o$, equivalent to $[10\bar{1}]_c$.

Within the streaking the presence of an extra spot was often observed, as indicated by an arrow in Fig. 5a. However, such extra spots were sometimes absent: a clear example is shown in Fig. 7a corresponding to a well-ordered crystal, as confirmed in Fig. 7b. The occasional presence of the extra spots, presumably due to multiple diffraction, suggests that, along the b_o axis, the unit cell may be the double of that given in the structural model of Grenier *et al.* (*8, 11*). Consequently, Figs. 2 to 7 were indexed on the basis of the larger cell, whose parameters are $a_c\sqrt{2} \times 6a_c \times a_c\sqrt{2}$. On the assumption that the doubling of the unit cell

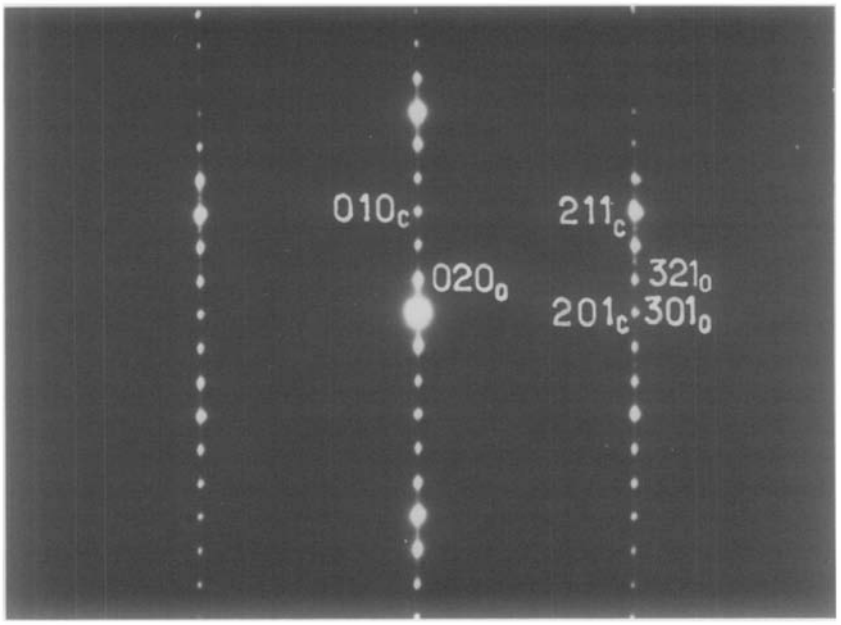

FIG. 3. Electron diffraction pattern of the L.T. orthorhombic sample. Zone axis $[10\bar{3}]_O \leftrightarrow [10\bar{2}]_C$.

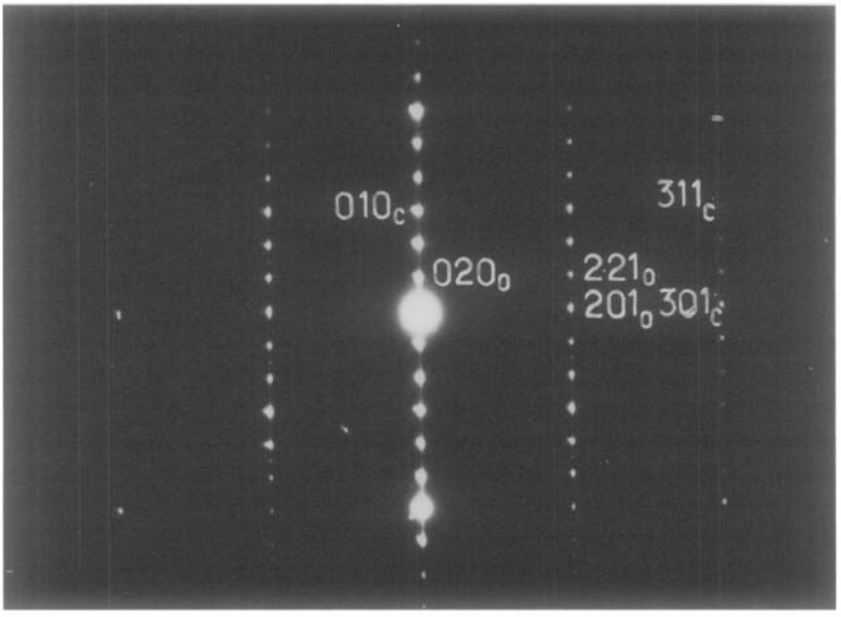

FIG. 4. Electron diffraction pattern of the L.T. orthorhombic sample. Zone axis $(10\bar{2}]_O \leftrightarrow [10\bar{3}]_C$.

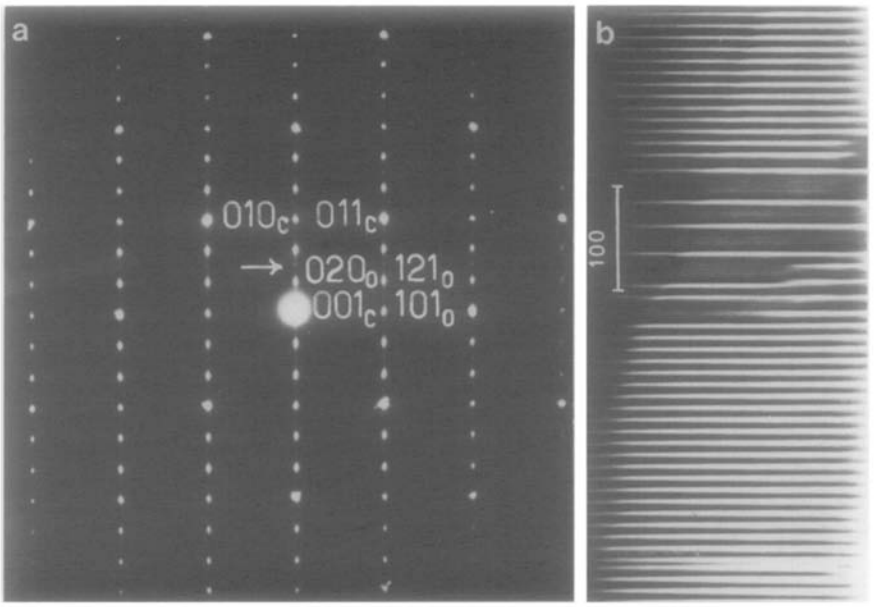

FIG. 5. (a) Electron diffraction pattern of the L.T. orthorhombic sample. Zone axis $[10\bar{1}]_o \leftrightarrow [100]_c$. Arrow signals the spots doubling the unit cell. Notice the streaking along the $b_c^* \leftrightarrow b_o^*$ axis. (b) Corresponding electron micrograph. The streaking shown in Fig. 5a is due to disordering (see text).

is due to an alternation in the orientation of the $[FeO_4]$ tetrahedra along the b_o axis, the idealized unit cell of this solid is shown in Fig. 1d. In this connection, it is worthwhile recalling that in the case of the brownmillerite-type structure (*9, 10*) (Fig. 1a), although the sequence of the polyhedra layers is . . .OTOTOT. . ., the b_B parameter is four times the perovskite cubic cell parameter, since the relative orientations of the tetrahedra alternate along this axis. The real sequence of the polyhedra layers may then be written . . .OTOT'OTOT'. . ., and the unit cell is approximately $a_c\sqrt{2} \times 4a_c \times a_c\sqrt{2}$.

In a similar way, Bando *et al.* (*13, 14*) have indexed the closely related $Ca_4YFe_5O_{13}$, another member of the Grenier *et al.* series of phases ($n = 5$) with an approximate cell $a_c\sqrt{2} \times 10a_c \times a_c\sqrt{2}$ corresponding to a sequence . . .OTOOTO T'OOT'O. . . .

Other explanations are, however, possible; to confirm this point, a HREM study of samples showing the extra spots will be useful.

Moreover, it is quite clear that, with such a structural building principle, an infinite number of different sequences and consequently of different structures and stoichiometries is "a priori" possible. Some of them have already been shown to exist by Grenier *et al.* When the intergrowths of the end members of the series are perfectly ordered, they give rise to new compositions and structures; when they are disordered they allow compositional variations to happen. Evidence of the last phenomenon appears in Fig. 5b, where one can measure interplanar spacings between 7.8 and 30.5 Å.

High-Temperature Sample (H.T.)

The chemical analysis of the sample treated at 1400°C in air indicated a composition $Ca_2LaFe_3O_{8.235} \Leftrightarrow Ca_{0.67}La_{0.33}FeO_{2.745}$

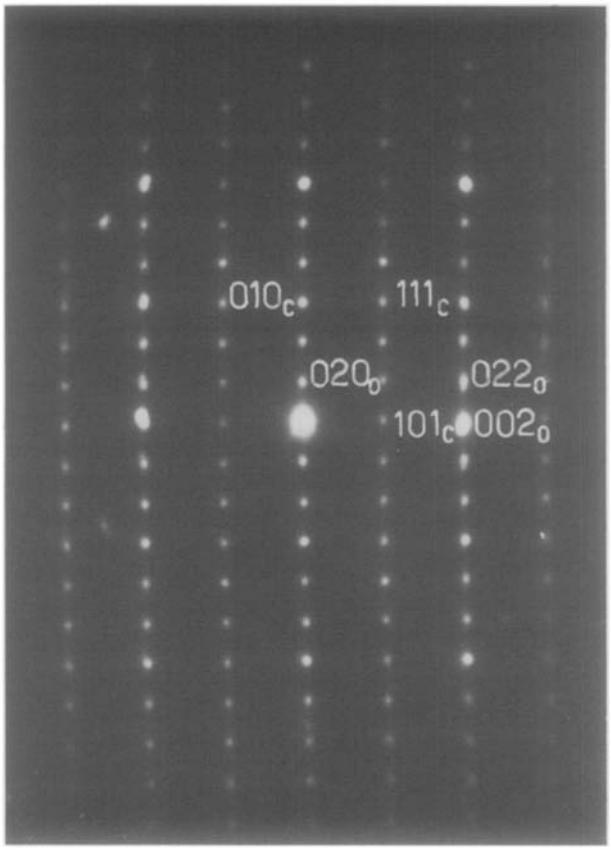

FIG. 6. Electron diffraction pattern of the L.T. orthorhombic sample. Zone axis $[100]_o \leftrightarrow [10\bar{1}]_c$.

(i.e., 15.6% Fe^{IV}). X-Ray powder diffraction data only showed interplanar spacings corresponding to a cubic perovskite-type cell with $a = 3.848(3)$ Å.

Electron diffraction, however, shows the existence of a much more complex situation.

Figure 8 shows an electron diffraction pattern along the $[001]_c$ zone axis indicating, besides the cubic perovskite reciprocal lattice, the presence of an additional spot at the center of the reciprocal cell. Even more interesting is the existence of threefold superlattices along both the a_c^* and b_c^* directions. Each of these two threefold superlattices is reminiscent of that found in the reduced low-temperature sample. Nevertheless, for this last sample, a threefold superlattice was present in only one direction (b_c^*, see Figs. 2 to 7).

A possible interpretation of the reciprocal lattice section appearing in Fig. 8 is that, within the same crystal, two different orientations of the . . .OOTOOTOOT. . . sequence are present. These two orientations would be perpendicular, as could be seen, for example, in a 90° twin. However, an electron micrograph of the same crystal in one of those orientations (Fig. 9) shows a much more complicated situation. It can be seen that the crystal is not really twinned; it is in fact formed by intergrowth of small domains, where the unit cell is tripled in one of the two perpendicular directions: either a_c or b_c, according to the indexing given in Fig. 8. The size of these regions is

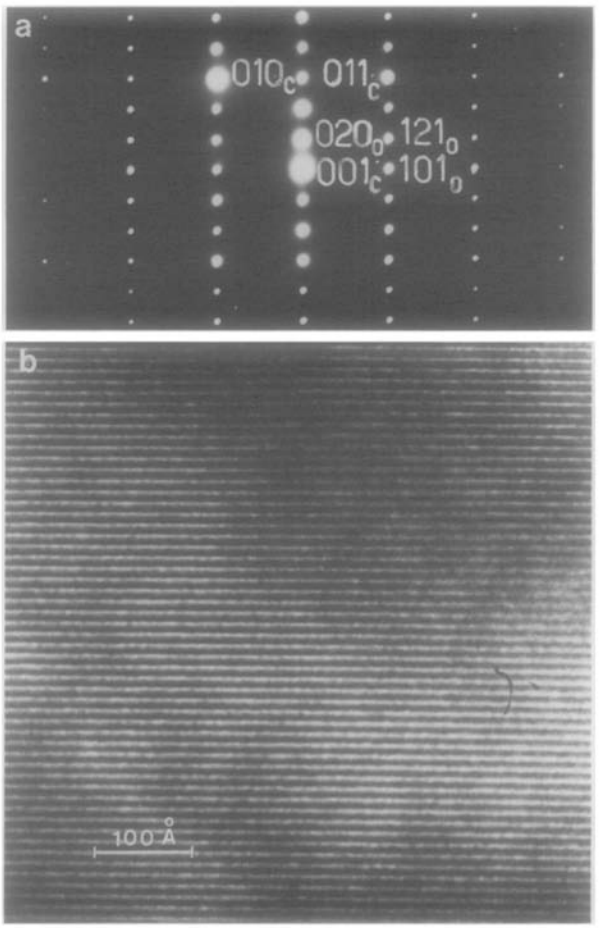

FIG. 7. (a) Electron diffraction pattern of a well-ordered crystal of the $Ca_2LaFe_3O_8$ sample. Zone axis $[10\bar{1}]_o \leftrightarrow [100]_c$. Notice the systematic absence of the spots (*hkl*) with $k = 2n + 1$. Compare with Fig. 5a. (b) Corresponding electron micrograph. Compare with Fig. 5b.

difficult to estimate accurately, but they are of the order of ~60 to ~100 Å in an approximately square block. In any case, given this order of magnitude of size, one can speak of these regions as *microdomains*. A set of microdomains, say, set α, will have the unit cell tripled in the a_c direction, while the other one, set β, has the unit cell tripled in the b_c direction. From the information so far available, these microdomains would appear to be two-dimensional, i.e., their third dimension is hitherto unknown and can be supposed as infinite.

In an attempt to understand more fully such an uncommon structural situation, a series of tilts were performed, on the same crystal, around the perovskite reciprocal b_c^* axis.

Figure 10 shows the $[10\bar{1}]_c$ zone axis, obtained after a tilt of 45°. This pattern can be fully indexed on the basis of the orthorhombic cell $a_c\sqrt{2} \times 3a_c \times a_c\sqrt{2}$ (or with the double cell obtained for the low-temperature sample; the smaller cell has in fact been used here for simplicity). Along this orientation both L.T. and H.T. samples

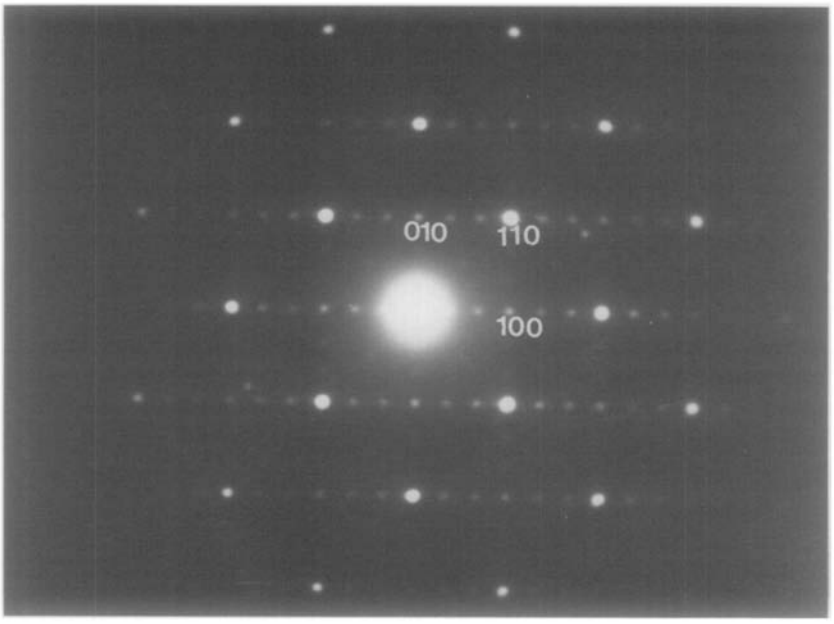

FIG. 8. Electron diffraction pattern of the H.T., X-ray cubic sample. Zone axis $[001]_c$. Notice the spot at the center of the reciprocal cubic cell (compare with Fig. 2) and the presence of two threefold superlattices along both $\bar{g}_{010}$ and $\bar{g}_{100}$.

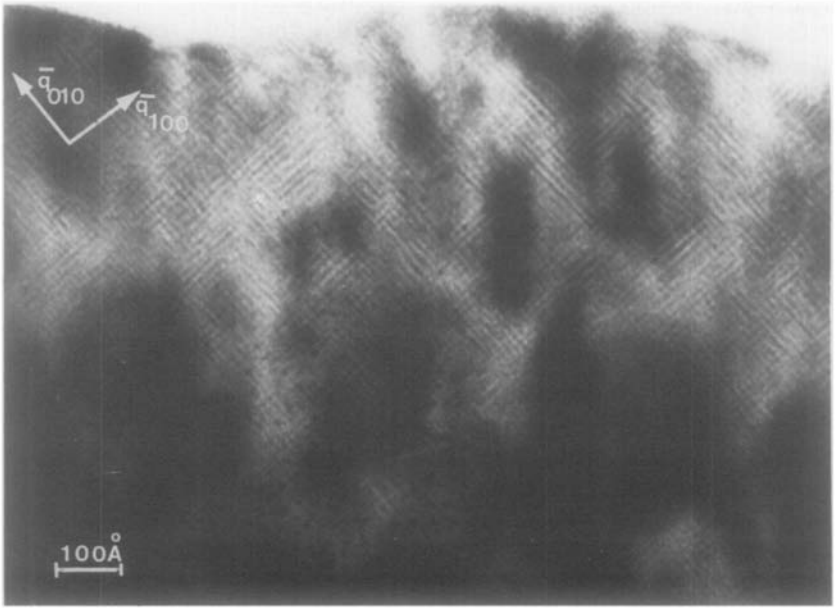

FIG. 9. Electron micrograph of the H.T., X-ray cubic sample, in the $[001]_c$ orientation of Fig. 8. The presence of microdomains, in which the perovskite cell is trebled in one of two perpendicular directions, is evident.

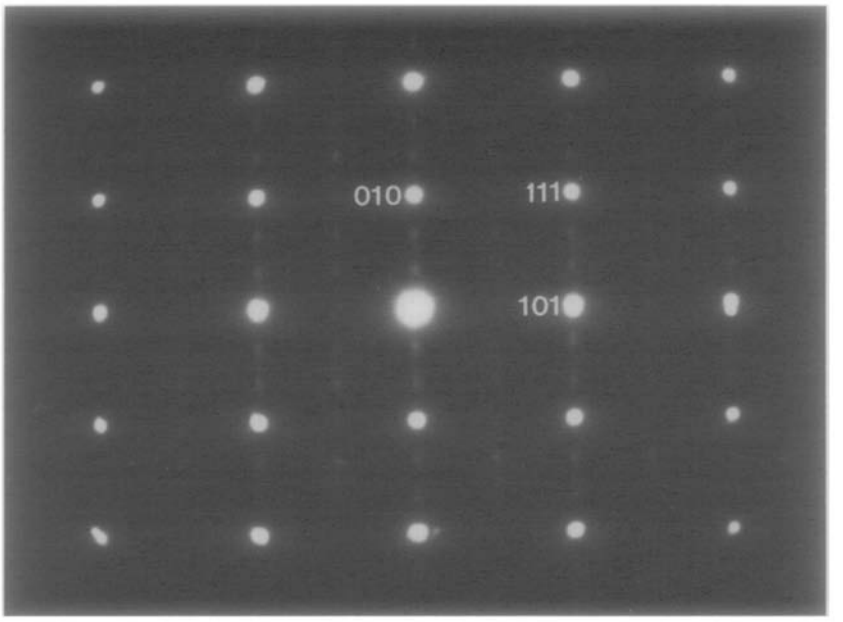

FIG. 10. Electron diffraction pattern of H.T., X-ray cubic sample; zone axis $[10\bar{1}]_c \leftrightarrow [100]_o$. Compare with Fig. 6 of the L.T. sample.

give geometrically similar diffraction patterns, but the intensities of the spots are clearly different. However, the $[10\bar{3}]_c$ zone axis (Fig. 11a) obtained after a tilt of 11.5° around the b_c^* reciprocal cubic axis, from the $[001]_c$ zone axis, is much more complex. The abundance of diffracted spots suggests that the reciprocal lattice is more complicated than that which could be deduced previously from Fig. 8. In particular the presence of the spots marked by the letters *A* and *B*, which can be indexed as $[1\ 0\ \frac{1}{3}]_c$ and $[2\ 0\ \frac{2}{3}]_c$ in the cubic perovskite cell, indicates that the cubic perovskite axis c_c^* also shows a threefold superstructure. This in itself implies that there exists a third group of microdomains in which the tripling of the unit cell happens in a direction perpendicular to that observed on the two sets whose existence was deduced from Figs. 8 and 9.

Coming back to Fig. 11a, the group of four spots forming a cross, marked by an arrow, corresponds to the intersection of the two threefold superstructures, parallel to a_c^* and b_c^*, within the reciprocal unit cell centered at $(\frac{3}{2}\ \frac{1}{2}\ \frac{1}{2})_c$, as schematically shown in Fig. 12a. All the spots present in Fig. 11a can then be indexed in the perovskite cubic cell as shown in Fig. 11b.

On the basis of all this information, it can be concluded that the high-temperature oxidized form $Ca_2LaFe_3O_{8+z}$ is composed of three sets of microdomains, which we can denote α, β, and γ, homogeneously intergrown within the same crystal. Each of these microdomains is actually related to, but not identical with, the low-temperature sample described in the previous section. That the low- and high-temperature samples are not structurally identical can be deduced from a comparison of Fig. 2 and Fig. 8: the L.T. sample is orthorhombic, and $a_o \neq c_o$ (Fig. 2), while the H.T. sample is, at least geometrically, tetragonal with two equal axes (Fig. 8) either $a_t = c_t$, $a_t = b_t$, or

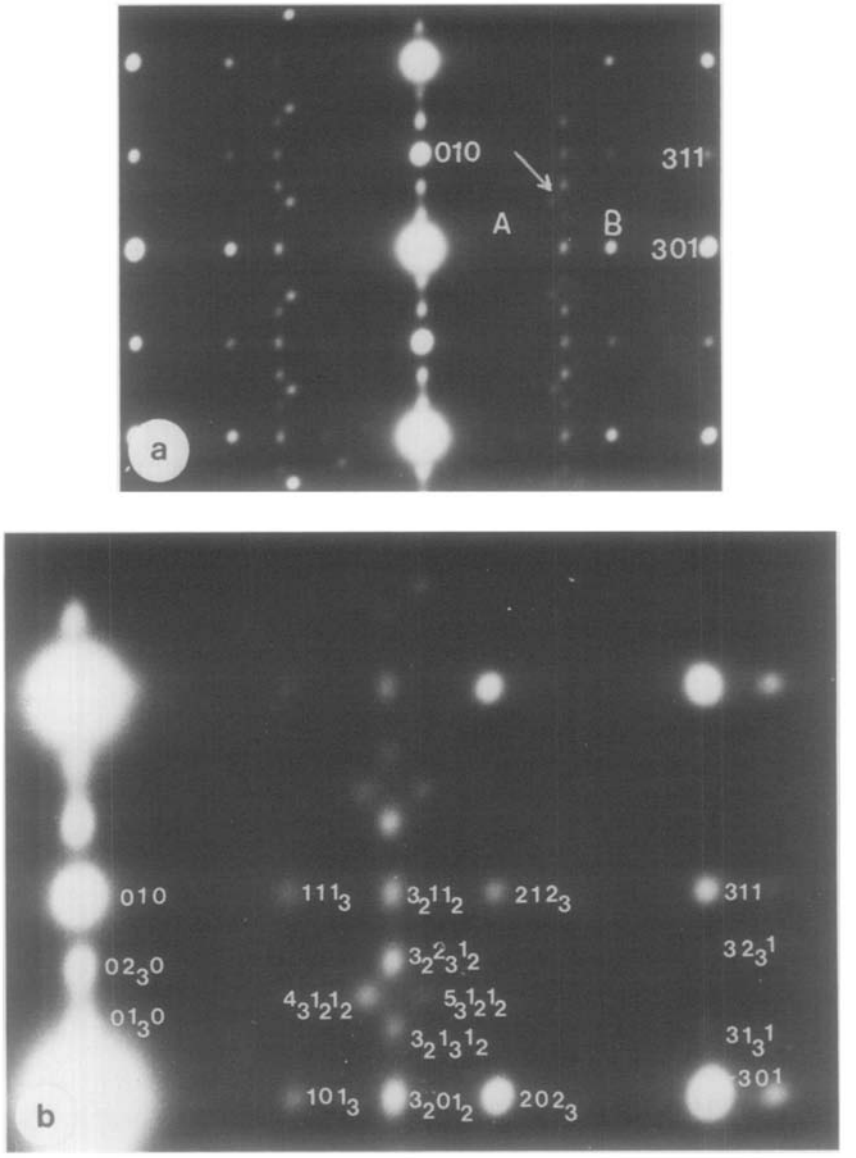

FIG. 11. (a) Electron diffraction pattern of the H.T. sample; zone axis $[10\bar{3}]_c$. The presence of the spots indicated by the letters *A* and *B* suggests that the unit cell is also trebled in the *c* direction. A ≡ $[1\ 0\ \frac{1}{3}]_c$, *B* ≡ $[2\ 0\ \frac{2}{3}]_c$ and equivalent. (b) Enlargement of the previous pattern, indexed on the basis of the perovskite cell (see Fig. 12a).

$b_t = c_t$ depending on the domain selected. This situation is perhaps due to the very presence of *a microdomain texture*.[3]

[3] The word *texture*—arrangement of the parts that make up something—is used here instead of structure to distinguish the structural arrangement of the whole solid from that of each microdomain.

As a consequence of this microdomain intergrowth, the reciprocal space corresponding to the high-temperature oxidized phase of $Ca_2LaFe_3O_{8.235}$, shown in Fig. 12a, is formed by the juxtaposition of three reciprocal spaces, given in Figs. 12b, c, and d, each of them corresponding to one set of

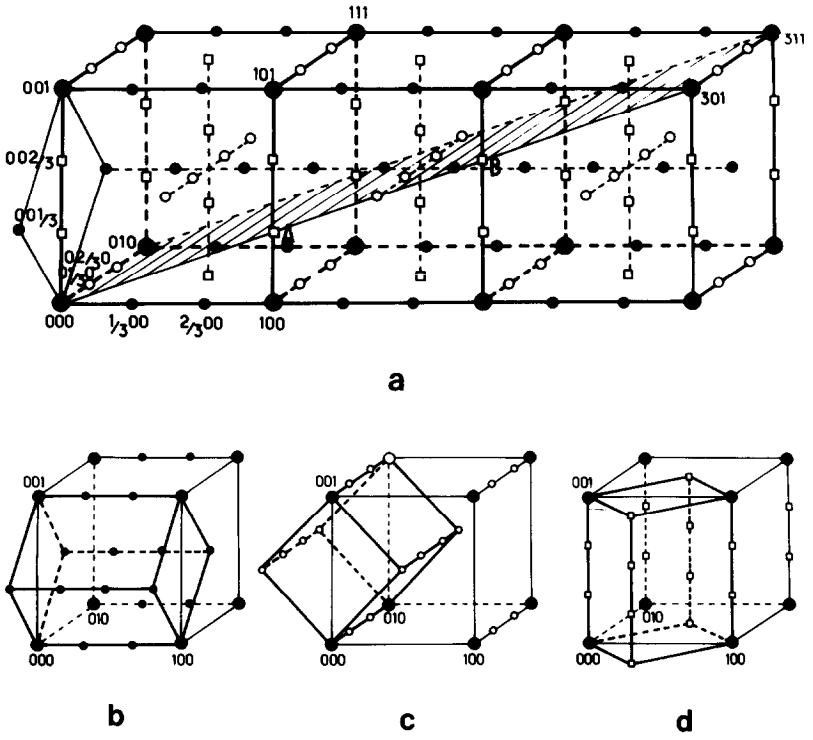

FIG. 12. (a) Schematic representation of a part of the reciprocal lattice of the H.T., X-ray cubic sample as observed by electron diffraction. Indexation is made on the basis of the cubic perovskite cell. The shadowed plane corresponds to the pattern pictured in Fig. 11. This reciprocal lattice results, in fact, from the juxtaposition of three reciprocal lattices, each corresponding to one set of domains represented in: (b) set α: $3a_c \times a_c\sqrt{2} \times a_c\sqrt{2}$; (c) set β: $a_c\sqrt{2} \times 3a_c \times a_c\sqrt{2}$; (d) set γ: $a_c\sqrt{2} \times a_c2 \times 3a_c$.

domains and having as unit cell parameters: set α: $3a_c \times a_c\sqrt{2} \times a_c\sqrt{2}$; set β: $a_c\sqrt{2} \times 3a_c \times a_c\sqrt{2}$; and set γ: $a_c\sqrt{2} \times a_c\sqrt{2} \times 3a_c$.

It should be emphasized that the real situation does not correspond to a simple perovskite structure trebled in the three space dimensions, but rather to a crystal in which some tridimensional domains have a perovskite cell tripled in the a_c direction, in other domains it is tripled in the b_c direction, and in the remaining ones the unit cell is tripled in the c_c direction. These microdomains are randomly intergrown, as schematically shown in Fig. 13.

Figure 14 shows another electron micrograph, in the same orientation $[001]_c$, in which the microdomains are clearly seen to be of three kinds. Obviously, along this orientation, no fringes can be seen on the set of microdomains in which the unit cell is trebled in the c_c direction.

Discussion

The results obtained confirm that the low-temperature reduced phase of the calcium–lanthanum ferrite, $Ca_{0.67}La_{0.33}FeO_{2.67}$, is the $n = 3$ member of a series of anion-deficient perovskites of general formulation $A_nM_nO_{3n-1}$ (*8*). In this particular case $A = (\frac{2}{3}Ca + \frac{1}{3}La)$, M = Fe, and $x = \frac{2}{3}$ in the $Ca_xLa_{1-x}FeO_{3-y}$ solid solution, $y = 1/n$. Streaking in the electron diffraction diagrams and electron microscopic observation of this sample showed the occurrence

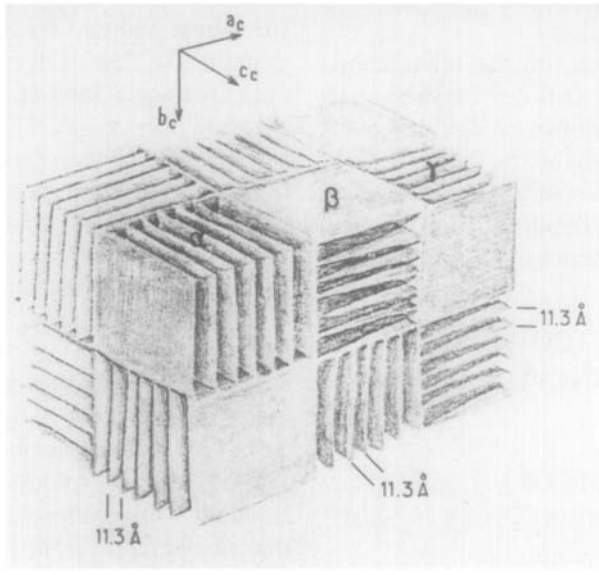

FIG. 13. Schematic representation of the intergrowth of three sets of domains which form the texture of the H.T. sample.

of some disorder along the b_o axis, parallel to the cubic perovskite b_c axis. As clearly shown in Fig. 6 by electron microscopy, the existence of fringe spacings larger than required by the b_o = 11.29-Å dimension was often observed. The appearance of such a

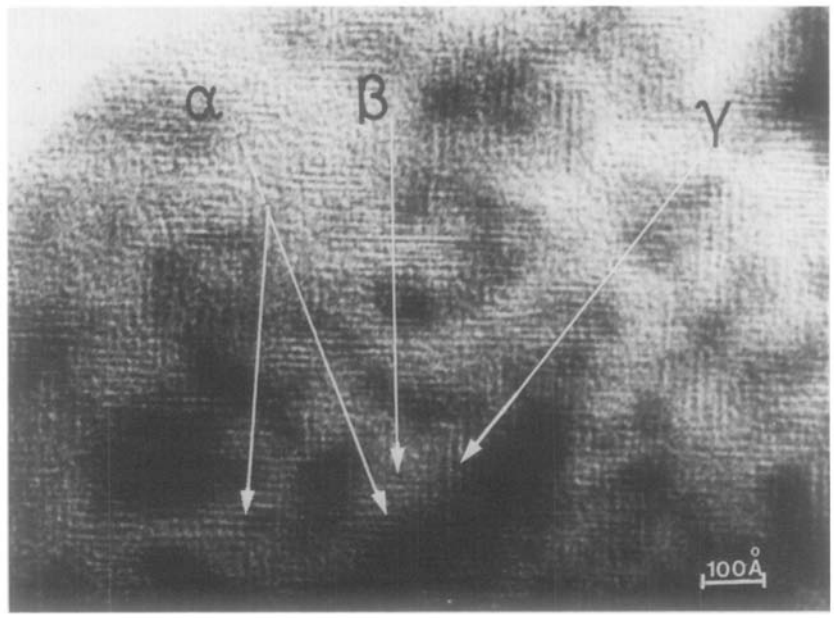

FIG. 14. Electron micrograph of the H.T. sample along the $[001]_c$ orientation showing the three sets of microdomains.

disorder supposes that the crystal is not in an equilibrium situation.

Electron diffraction, on the other hand, shows that the unit cell corresponding to this phase can sometimes be doubled compared to that predicted by the model of Grenier *et al.* (*8, 11*). This seems to suggest the existence of two polymorphic forms. The corresponding sequences of "polyhedra layers" would be:

I . . .OOTOOT'OOTOOT'. . .,
with a unit cell $a_c\sqrt{2} \times 6a_c \times a_c\sqrt{2}$,

and

II . . .OOTOOTOOTOOT. . .,
with a unit cell $a_c\sqrt{2} \times 3a_c \times a_c\sqrt{2}$.

As both species correspond to the same composition and as their respective structures are formed by the same structural elements stacked in different ways along one direction (the b_c perovskite axis), they could actually be *polytypes*. Idealized structural models of both polytypes appear in Figs. 1c and d.

The most interesting situation is found, however, in the high-temperautre oxidized sample, whose "average structure" as observed by powder X-ray diffraction appears to have a cubic cell with $a = 3.848(3)$ Å.

Nevertheless, as clearly demonstrated by the combination of both electron microscopy and diffraction, the real structure of such a material is formed by intergrowth of three families of microdomains.

Although three-dimensional microdomain intergrowth within a perovskite-like phase have recently been found in the closely related $Sr_xNd_{1-x}FeO_{3-y}$ system (*15*), the structure within each domain was not established unambiguously. Nevertheless, the available diffraction evidence suggested, in that case, a perovskite unit cell *doubled* in one of the three axes alternating at random in each domain. In the present case, however, there exists a close analogy between the structure of the low-temperature phase and that observed for each set of domains, so that each of the microdomains appears to be a kind of tetragonal low-temperature polymorph. The existence of a material having a *microdomain texture* raises a number of problems regarding the definition of a phase and also concerning the ways in which nonstoichiometry can be accommodated. Some of these problems have recently been discussed (*16*) and reviewed (*17*).

It appears that the concept of microdomains was first used by Ariya and Morozova (*18*) to explain physicochemical and, in particular, thermodynamic properties of titanium, vanadium, or iron monoxides. In one of their first contributions to the subject, regarding wüstite, Ariya and Morozova suggested the existence of microdomains of a structure type, say, α, within the structure of a parent solid, say, β. Ariya and Morozova described a "FeO lattice in which islands of agglomerates of Fe^{III} are disseminated . . . ." Such a situation implied the existence of a "submicroinhomogeneous structure." Later, however, Ariya and Popov (*19*) considered that the nonstoichiometric solid, say, A, was composed of coexisting microdomains of two phases, say, B and C, both of which are adjacent to A in the phase diagram. As for the reason why B and C have a different composition, the compositional variation of the A phase will actually be a reflection of the evolution of the relative amounts of B and C: in this respect, the thermodynamic behavior of A will be univariant. The absence of superlattice lines in the X-ray diffraction diagrams of those solids indicated, according to Ariya and Popov (*19*), "the statistically random distribution of the domains with compositions B and C in the lattice of this oxide."

As already pointed out by Banks (*20*), the problem raised by this interpretation is that, near each side of the homogeneity

range, one should see on the X-ray diffraction pattern the lines corresponding to the predominating B or C phase superimposed on those of the matrix; those lines are, however, not visible.

Nevertheless, by dark-field electron microscopy microdomains have been observed in a few examples. In particular, both TiO_x and VO_x have been shown to at least partly fulfill what is usually referred to as the "Ariya hypothesis" (*21*). Watanabe *et al.*, (*22*) were able to image interesting microstructural features and, in particular, two-dimensional domains in the form of parallel plates, of ~300–1000 Å thickness, in several samples of "titanium monoxide" (*22*). On the other hand, Bell and Lewis have observed in "vanadium monoxide" domains of a tetragonal superlattice where the tetragonal axis may be selected from one of the three cubic unit cell axes of the matrix (*23*).

The case that we are referring to, however, appears to be somewhat different in that there is no evidence of the matrix. That we can really observe simultaneously the diffraction patterns of both the parent and the domain structures is only due to the fact that the latter is a superstructure of the former. However, in the electron microscope images, the whole observation field is fully occupied by the three sets of microdomains (see Figs. 9 and 14). These facts bring us to a second worthwhile point. It concerns the size of the domains and, in close connection with it, the amount of order within them. With respect to the first aspect, simple calculations by Ariya and Popov (*19*) suggested a domain side of the order of 3 and 9 unit cells in the case of TiO, which means ~30 to 1000 unit cells within a domain, depending on the composition. A more elaborate treatment of the problem within the thermodynamic criteria for small systems allowed Anderson (*17*) to obtain a much smaller figure: 5 to 7 unit cells/domain in the case of $CeO_{1.94}$, while in the case of UO_{2+x} the domain size could be as small as one unit cell, i.e., disordered Willis clusters. As measured in Fig. 9, we can obtain an approximate domain size of the order of 6 to 10 times b_o, i.e., 6 to 10 unit cells on one side, which in the supposition of the domains being isometric blocks or islands—something which is not totally evident in Fig. 9—could mean a microdomain volume of the magnitude of 200 to 1000 unit cells. The agreement with Ariya's value is likely to be fortuitous. However, an interesting point concerning the three-dimensional domains observed in the calcium–lanthanum ferrite is that the absence of the matrix indicates that each domain tends to occupy the maximum available volume. This in itself implies, on the one hand, that the observed microdomain individual volume is as big as possible, which is compatible with the homogeneity of the domain size. But this also indicates that the microdomains result in this case from a "randomization" of the oxygen excess. It is worthwhile to stress in this connection that microdomains appear in the calcium–lanthanum ferrite as a result of a high-temperature ($T \sim 1400$°C) oxidation process, while in the other known cases (*22, 23*) they occur in the process of relatively low temperature annealing (e.g., 600–700°C in VO_x). That the microdomain textured solid is a quenched high-temperature solid is confirmed by the fact that annealing in air at low temperatures produces mixed crystals of the L.T. and H.T. materials (*24*).

Closely related with the question of the domain size is the problem of ordering within the domains (*17*). In view of the diffraction properties of the high-temperature oxidized phase we can speak of these microdomains as long-range ordered. On the contrary, where short-range ordering predominates, diffuse scattering is observed. A typical case of such a situation concerns the Cu_3Au alloys, where Moss (*25*) deduced from the diffuse scattering a domain

size of about 6 × 3 × 3 unit cells. It must be noticed, however, that Moss's analysis refers to an order–disorder phenomenon where no global compositional variations are observed.

A more interesting and related case concerns the anion-deficient fluorite-type phases based on zirconia and hafnia studied by Allpress and Rossell (*26*). In this case, diffuse scattering was shown to be due to small domains embedded coherently in a number of specific orientations within the cubic matrix. After long annealing times the ordering process originates a superlattice (*26*).

On the other hand, and against what has been observed in A-cation-deficient perovskites showing two-dimensional domains (*27*), no ordering between domains has been observed in the calcium–lanthanum ferrite. The distribution of domains, i.e., the orientation of the long b_0 axis, is random. It is possible that long annealing times at 1400°C could order the domains.

Perhaps the more crucial question regarding the microdomain textured materials concerns their classification as a phase. According to the usual definition (*28*), a *phase* is a region of matter within which all microscopic properties vary continuously as a function of position, while a *uniform phase* is a region within which all properties are independent of position. It would then appear that each of the observed microdomains, excluding the domain walls, can be considered as a uniform phase; however, the global, textured solid is not a uniform phase, nor even a phase in the sense indicated above. Such a microdomain ensemble is perhaps more akin to the *hybrid crystal* concept postulated by Ubbelohde (*29*) in the case of phase transformations, or to the otherwise probably equivalent (*30*) concept of *pseudophase* (*31*) postulated by Hyde *et al.* to explain the thermodynamic behavior of the Pr–O_2 system.

Nevertheless, the concept of phase can alternatively be considered, at least in operational terms, on the basis of two criteria, proposed long ago by Anderson (*32*) in the context of nonstoichiometry. Such criteria concern a phase within the broader scope of compositional variations, and can be summarized as follows: a nonstoichiometric phase has to be *structurally monophasic*—as determined by a diffraction technique, usually powder X-ray diffraction—and *thermodynamically bivariant*. As suggested in the model of Grenier *et al.* (*8, 11*), the ratio of octahedra to tetrahedra controls the compositional variations of these AMO_{3-y} ferrites: when the sequence is ordered, it leads to different terms of the series; if it is disordered, it originates local compositional variations. The low-temperature phase described above gives an example of the last type. However, the nature of the high-temperature oxidized phase indicates that this is not the way in which nonstoichiometry is accommodated in air at 1400°C, in the mixed-calcium–lanthanum ferrite, since in no case have we observed at that temperature any interplanar spacing longer than the expected b_0 = 11.29 Å within the microdomains. This seems to imply that in this case the domain walls play a decisive role in accommodating the oxygen excess. If this reasoning is correct, the greater the domains the smaller will be the oxygen excess.

Concluding Remarks

The results shown above indicate that three-dimensional microdomain formation is yet another way of accommodating compositional variations in solids. In this particular example, an excess of oxygen appears to be accommodated in the domain walls, suggesting that different compositions may give rise to different domain sizes.

Although the observation of three-dimensional microdomains constitutes a new de-

velopment in nonstoichiometry, it actually raises more questions than it provides answers for. Some of these problems have already been discussed by Cowley in theoretical terms (*33*) and a new theoretical approach to the microdomain model has recently been put forward by Manes (*34*). One of the most critical issues to be explained is the true origin of the microdomains and, in a more general way, why some materials accept changes in composition by accommodating point defects, some by defect complexes, others by an extended defect mechanism, others by ordered or disordered intergrowths, and others by microdomain formation. Even more so, the calcium–lanthanum ferrite appears to conform to one or the other of the last two types depending on the temperature at a given oxygen pressure.

It is also clear that the presence of microdomain walls will have a strong influence on the physicochemical properties, and in particular on the transport features of this type of solid. Whether this goes as postulated by Van Gool and Bottelberghs (*35*) some years ago, in a model that is in some respects an extension of the Ariya hypothesis, remains to be tested.

Acknowledgments

We thank Louis Puebla and Alfonso Garcia for technical assistance.

References

1. J. S. ANDERSON, Shear structures and non-stoichiometry, *in* "Surface and Defect Properties of Solids" (J. M. Thomas and M. W. Roberts, Eds.), p. 31, The Chemical Society, London (1972).
2. B. T. M. WILLIS, *Acta Crystallogr. Sect. A* **25,** 277 (1969).
3. L. A. BURSILL AND B. G. HYDE, "Progress in Solid State Chemistry" (H. Reiss and J. O. McCaldin, Eds.),, Vol. 7, p. 177, Pergamon, Oxford (1972).
4. R. J. D. TILLEY, *Mater. Res. Bull.* **5,** 813 (1970).
5. B. HYDE, *in* "The Chemistry of Extended Defects in Non-metallic Solids" (L. Eyring and M. O'Keeffe, Eds.), p. 377, North-Holland, Amsterdam (1970).
6. J. S. ANDERSON AND R. J. D. TILLEY, Crystallographic shear and non-stoichiometry, *in* "Surface and Defect Properties of Solids" (M. W. Roberts and J. M. Thomas, Eds.), Vol. 3, p. 37, The Chemical Society, London (1974).
7. J. C. GRENIER, Thesis, Université de Bordeaux (1976).
8. J. C. GRENIER, J. DARRIET, M. POUCHARD, AND P. HAGENMULLER, *Mater. Res. Bull.* **11,** 1219 (1976).
9. E. F. BERTAUT, P. BLUM, AND A. SAGNIERES, *Acta Crystallogr.* **12,** 149 (1959).
10. J. BERGGREN, *Acta Chem. Scand.* **25,** 3616 (1971).
11. J. C. GRENIER, G. SCHIFFMACHER, P. CARO, M. POUCHARD, AND P. HAGENMULLER, *J. Solid State Chem.* **20,** 365 (1977).
12. J. C. GRENIER, F. MENIL, M. POUCHARD, AND P. HAGENMULLER, *Mater. Res. Bull.* **12,** 79 (1977).
13. Y. BANDO, H. YAMAMURA, AND Y. SEKIKAWA, *J. Less-Common Met.* **70,** 281 (1980).
14. Y. BANDO, Y. SEKIKAWA, H. YAMAMURA, AND Y. MATSUI, *Acta Crystallogr. Sect. A* **37,** 723 (1981).
15. M. A. ALARIO-FRANCO, J. C. JOUBERT, AND J. P. LEVY, *Mater. Res. Bull.*, **17,** 733 (1982).
16. General discussion reported in Ref. (*5*).
17. J. S. ANDERSON, *in* "Problems of Non-stoichiometry" (A. Rabenau, Ed.), p. 1, North-Holland, Amsterdam (1970).
18. S. M. ARIYA AND M. P. MOROZOVA, *J. Gen. Chem.* (*URSS*) **28,** 2647 (1958).
19. S. M. Ariya and Y. G. Popov, *J. Gen. Chem.* (*URSS*) **32** (7), 2054 (1962).
20. E. BANKS, Ref. (*5*), p. 16.
21. T. M. ADAMS, "Inorganic Solids," Chap. 9, p. 283, J. Wiley, New York (1974).
22. D. WATANABE, O. TERASAKI, A. JOSTSON, AND J. R. CASTLES, Electron microscopy study on the structure of low temperature modification of titanium monoxide phase, Ref. (*5*), p. 238.
23. P. S. BELL AND H. M. LEWIS, *Phys. Status Solidi A* **7,** 431 (1971).
24. M. VALLET AND M. J. R. HENCHE, unpublished results (1981).
25. S. C. MOSS, *J. Appl. Phys.* **35,** 3547 (1964).
26. J. G. ALLPRESS AND H. J. ROSSELL, *J. Solid State Chem.* **15,** 68 (1975).
27. M. A. ALARIO-FRANCO, I. E. GREY, J. C. JOUBERT, H. VINCENT, AND M. LABEAU, *Acta Crystallogr., A* **38,** 177 (1982).

28. H. F. FRANZEN, *Acta Chem. Scand.* **17,** 2341 (1963).
29. A. R. UBBELOHDE, *J. Chim. Phys.* **62,** 33 (1966).
30. B. G. HYDE, Ref. (5), p. 654.
31. B. G. HYDE, D. J. M. BEVAN, AND L. EYRING, *Philos. Trans. Roy. Soc. London Ser. A* **259** (1966).
32. J. S. ANDERSON, *Proc. Roy. Soc. Ser. A* **185,** 69 (1956).
33. J. M. COWLEY, The structure and ordering of microdomains, *in* Ref. (5), p. 259.
34. L. MANES, *in* "Non-Stoichiometry Oxides" (O. T. Sorensen, Ed.), Chap. 3, p. 100, Academic Press, New York (1981).
35. W. VAN GOOL AND P. H. BOTTELBERGHS, *J. Solid State Chem.* **7,** 59 (1973).